

# Reconstructing meteoroid trajectories using BRAMS data

Hervé Lamy<sup>1</sup>, Joachim Balis, Michel Anciaux

This paper summarizes our recent efforts in retrieving meteoroid trajectories using data from the forward scatter radio system BRAMS. Two methods are presented, one based only on the knowledge of time delays measured between meteor echoes observed at various receiving stations, and one including information from a radio interferometer in addition to the time delays measurements. For comparison about the quality of trajectory reconstruction, data from the optical CAMS-BeNeLux network are used. A third method is briefly presented assuming the total range traveled by the radio wave is known at all receiving stations. This work contains only preliminary results available at the end of summer 2021. Discussions about improvements are provided at the end of the paper.

Received 2022 January 10

This work has been presented at the International Meteor Conference 2021 (held online).

## 1 Introduction

The BRAMS (Belgian RAdio Meteor Stations) network is a Belgian project using forward scatter of radio waves to detect and characterize meteoroids. It comprises a dedicated transmitter located in the South-West of Belgium and 38 receiving stations spread all over the Belgian territory and neighbouring countries (see Figure 1 for status in September 2021).

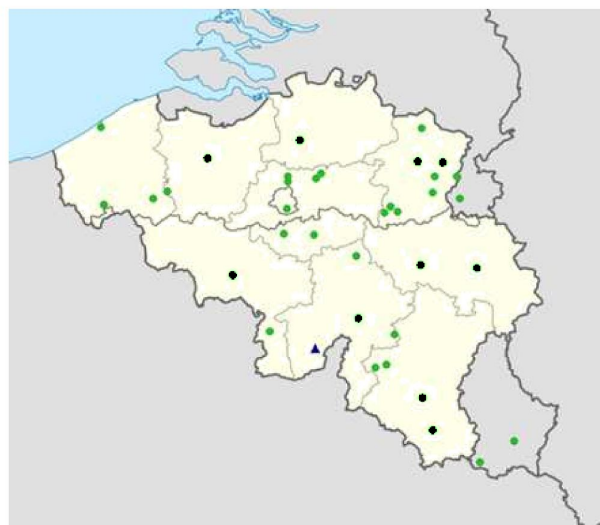


Figure 1 – Map of the BRAMS network in September 2021. The blue triangle is the transmitter located in Dourbes while the green dots are the 38 active receiving stations at the time.

The transmitter emits a circularly polarized continuous radio wave with no modulation at a frequency of 49.97 MHz with a power of 130 watts. All the receiving stations are using a 3-element Yagi antenna set-up vertically and trained in azimuth on the transmitter. In September 2021, approximately half of the receiving stations were using analog ICOM-R75 receivers, an

<sup>1</sup>Royal Belgian Institute for Space Aeronomy, Brussels, Belgium. Email: herve.lamy@aeronomie.be

external sound card to sample the signal coming from the receiver, and were controlled by the freeware program Spectrum Lab running on a Windows PC (see e.g. Lamy et al., 2015). The other half uses digital SDR-RSP2 receivers controlled by a Linux system running on a Raspberry Pi (Anciaux et al., 2020). All stations are equipped with a Garmin GPS that provides timestamps to the BRAMS data and allows a time synchronization between the receiving stations. Additional features of the receiving stations are not described here and we refer the reader to previous publications in the Proceedings of the IMC. A paper is also in preparation to describe the BRAMS network and data in full detail.

One of the difficulties with forward scatter systems is the determination of individual meteoroid trajectory and speed as the geometry is more complex than in the case of backscatter systems. In the specific case of BRAMS, the absence of modulation in the CW transmitted signal does not allow to estimate the total range traveled by the radio wave between the transmitter (Tx), the reflection point and the receiver (Rx), and therefore makes the problem even more complex. We present here an attempt to retrieve meteoroid trajectories using BRAMS data. Two methods are considered: one based only on measurements of time delays between meteor echoes recorded at different receiving stations, and one using the same data but complemented with data from the radio interferometer located in the Humain station which provides the direction of one specular reflection point. A (currently) hypothetical method is also presented assuming that the total range traveled by the radio wave is known for all receiving stations. In order to assess the quality of the reconstruction, a comparison with data from the CAMS-BeNeLux network is provided.

## 2 Two methods to determine meteoroid trajectory and speed

The first method (hereafter called Method 1) is based purely on geometrical considerations and relies on the specularity condition of the reflection of the radio wave. The specular reflection point is the point along the meteoroid path for which the total distance traveled by the radio wave is minimum, which means that the total distance  $S_i = R_{T_i} + R_{R_i}$  must be minimum for each receiving station  $i$ . Because the geometry Tx-

Trajectory number	Date	$T_{\text{beg}}$ hh:mm:ss	$V_{\infty}$ km/s	$X_{\text{Hum}}$ km	$Y_{\text{Hum}}$ km	$Z_{\text{Hum}}$ km
79	29/07/2020	23:14:00	41.96	45.24	57.95	95.37
105	29/07/2020	23:36:28	41.83	122.45	93.60	99.97
149	30/07/2020	00:17:18	26.45	-89.21	92.87	89.48
188	30/07/2020	00:51:27	29.95	-52.92	21.33	88.48
282	30/07/2020	01:44:28	40.59	-96.02	35.01	88.70
477	30/07/2020	22:07:58	61.36	-80.56	7.74	102.12
532	30/07/2020	22:56:54	36.90	39.56	50.58	92.07
536	30/07/2020	23:06:55	65.07	22.62	199.53	106.10
598	30/07/2020	23:43:54	70.46	6.91	158.72	103.19
654	31/07/2020	00:21:21	15.49	67.98	10.19	80.15
709	31/07/2020	00:48:40	63.70	-32.89	108.71	95.53
773	31/07/2020	01:25:38	65.68	-94.82	62.32	96.97

Table 1 – Selected CAMS trajectories used for comparison with the reconstructed trajectories using BRAMS data.  $T_{\text{beg}}$  is the begin time of the visual CAMS observation.  $V_{\infty}$  is the speed of the meteoroid at the top of the atmosphere.  $X_{\text{Hum}}$ ,  $Y_{\text{Hum}}$ , and  $Z_{\text{Hum}}$  are the coordinates of the specular reflection point for the Humain station in a Cartesian referential centered on the Dourbes transmitter. X is directed East-West and counted positive towards East, Y is directed North-South and counted positive towards North.

$Rx_i$  is different for each receiving station  $Rx_i$ , the corresponding reflection points will be located at various positions along the meteoroid path. This is illustrated in Figure 2 for a reference station  $Rx_0$  and another station  $Rx_i$ . In this example, the specular reflection point  $P_0$  for the reference station is created before the corresponding reflection point  $P_i$ . The distance between the two points depends on the speed of the meteoroid which is here assumed constant. As a consequence, the reference station will detect a meteor echo shortly before receiving station  $i$ , the time delay between meteor echoes depending on the meteoroid path and speed.

A meteoroid trajectory can be defined by the 3D Cartesian coordinates of one point (the one corresponding to a reference station) and the three components of the velocity which provides the direction (assuming again a constant speed). This gives a total of six unknowns (respectively called  $X_0$ ,  $Y_0$ ,  $Z_0$ ,  $v_x$ ,  $v_y$  and  $v_z$ ) and therefore the need to have at least six equations. In Method 1, these equations are provided by the fact that the total derivative,  $dS_i/dt$ , must be equal to 0 for at least six stations  $i = 1, \dots, 6$ . The mathematical details will be provided elsewhere. This leads to a set of  $\geq 6$  non-linear equations which contains the 6 un-

knowns and the time delays  $\Delta t_i$  between meteor echoes recorded at station  $i$  and the reference station. A non-linear solver must then be used to solve this set of equations and to take into account additional constraints on the unknowns, such as the height of all reflection points which must lie between e.g. 85 and 110 km altitude, or the speed of the meteoroid which must be larger than  $\sim 11$  km/s.

Note that a similar technique has been developed recently for CMOR (Mazur et al., 2020) but the authors use two additional assumptions that simplify the set of non-linear equations. The first is that the reference receiving site is a backscatter system, which leads to the condition  $\vec{r}_0 \cdot \vec{v} = 0$  where  $\vec{r}_0$  is the vector linking the transmitter to the reference reflection point. The second assumption is that the remote sites are rather close to the transmitter (distances  $\leq 20$  km). These two assumptions allow to simplify the set of non-linear equations into a set of linear equations for only the 3 components of the velocity. Unfortunately, neither of these assumptions are valid for the BRAMS network and we have therefore to solve the complete set of non-linear equations.

The second method (hereafter called Method 2) is using the same assumptions as Method 1 but includes data from our interferometric radio station located in Humain. Unlike the other receiving stations, it uses 5 antennas in the so-called Jones configuration (Jones et al., 1998; Lamy et al., 2018) and allows to determine the direction of arrival of the meteor echo to within approximately  $1^\circ$ . The interferometer provides two more equations for the azimuth and elevation of the specular reflection point but does not provide its exact position. With these additional equations, we only need time delays measured between 3 additional stations and a reference station in order to get at least 6 equations.

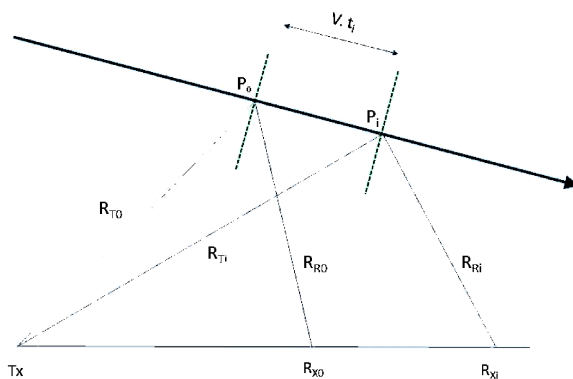


Figure 2 – Geometry of the problem for Method 1.

### 3 Validation procedure

To validate the reconstruction of the trajectory using BRAMS data and Method 1 or 2, optical data com-

ing from the CAMS BeNeLux network are used (Jenniskens et al., 2011; Roggemans et al., 2016). BIRA-IASB is a member of this network and provides daily data from 4 cameras. Data were provided for 2 clear consecutive nights from 29 to 31 July 2020, in a period without any strong activity from meteor showers. Among the 948 available trajectories, a selection was made based on the following criteria : (i) most of the trajectories are not located above Belgium and therefore not geometrically suitable to be detected by our BRAMS receiving stations, (ii) each trajectory must be detected by at least 6 stations, otherwise we reject it, (iii) because we want to compare Methods 1 & 2, one of these stations must be the interferometer in Humain, and (iv) we restrict ourselves as much as possible to underdense meteor echoes in order to ensure that the specular condition is valid. The application of these criteria resulted in a selection of 12 suitable CAMS trajectories. The parameters of these trajectories are summarized in Table 1.

The three coordinates of the reflection point for the reference station in Humain are computed knowing the trajectory (e.g. Lamy et al., 2016). Together with the 3 velocity components (projections of  $V_\infty$  along the trajectory, from CAMS data, onto the reference frame centered on Dourbes), they constitute our six unknowns to retrieve the meteoroid trajectory and speed.

#### 4 Determination of time delays

In the frame of the BRAMS network, the only measurements available are the time delays measured between the start of a meteor echo at various receiving stations and that at the reference station. The start of the meteor echo is chosen as the time when it rises to half the peak power. This should indeed correspond to the instant at which the specular reflection occurs. This process is done using only underdense meteor echoes, which therefore avoids using a possible additional larger maximum later on in the case of an overdense meteor echo.

Meteor echoes are first identified in the BRAMS spectrograms based on their approximate expected time of appearances which correspond to the passage of the meteoroid at the reflection points. These times are computed based on the initial time and height of the CAMS trajectory, and on the speed of the meteoroid. A visual inspection was done for this study to avoid selecting another meteor echo randomly appearing at approximately the same time. An automatic procedure is planned for this task in the future. Once the meteor echoes have been identified in the spectrograms, their frequency range can be computed automatically (see top panel of Figure 3). If this frequency range contains the frequency of the direct signal coming from the transmitter, the latter is first reconstructed using a local (i.e. computed every 5 seconds) FFT and then subtracted from the raw data (see middle panel of Figure 3). A Blackman filter of high order is then used to remove the noise at frequencies where the meteor echo does not appear. After these two steps, an accu-

rate determination of the start of the meteor echo can be computed on the power profile (see bottom panel of Figure 3).

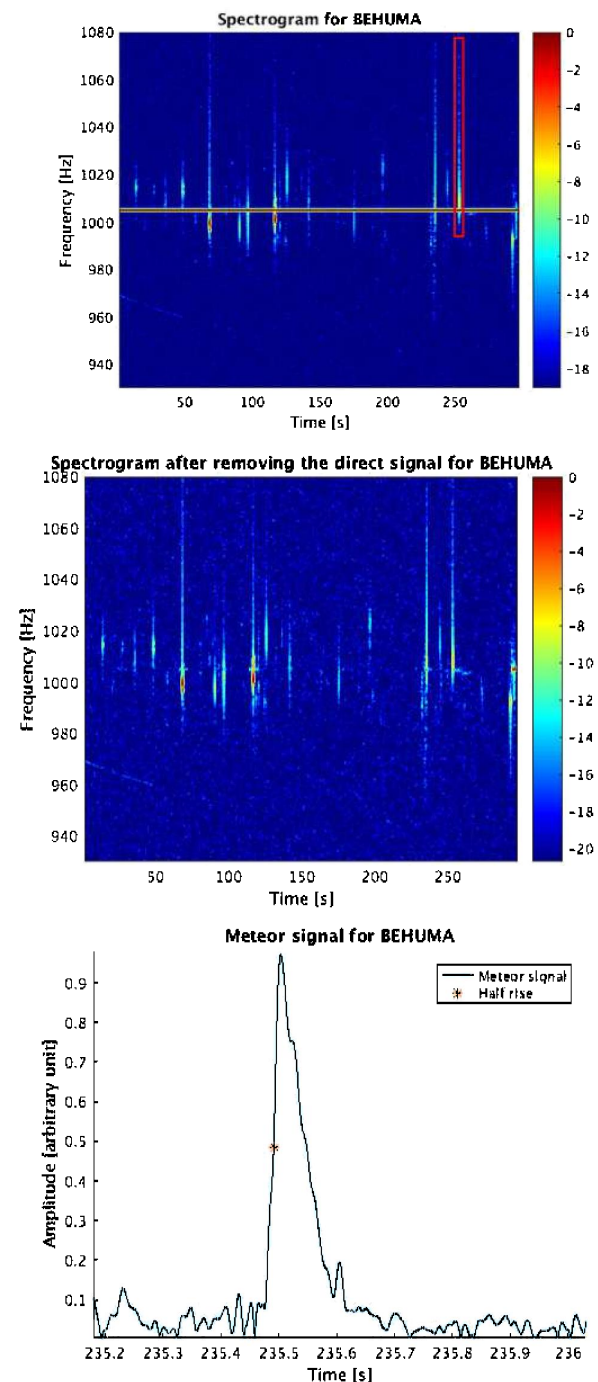


Figure 3 – Top Panel: Example of one meteor echo corresponding to CAMS trajectory 598 detected in the spectrogram of Humain (red rectangle). Middle Panel : same spectrogram obtained after subtracting the reconstructed direct signal coming from the transmitter from the raw data. Bottom panel : power profile of the meteor echo obtained after filtering all frequencies not included in the red rectangle. The time corresponding to half-peak power in the rising edge of the echo is marked.

## 5 Preliminary results

The results presented here were obtained during a master thesis organized at the University of Liège with supervision from the BRAMS team, and represent the work in progress on this topic at the time of the online International Meteor Conference organized in September 2021.

Codes were written in Matlab. The solver used to resolve the set of non-linear equations described in Section 2 was “lsqnonlin” which searches for the set of unknowns that minimizes the sum of the squares of the non-linear equations  $dS_i/dt = 0$ . This approach was not completely appropriate as this solver does not allow the application of constraints on some of the parameters (height of the specular reflection point and total speed of the meteoroid) in a simple way. Moreover, the target objective trying to minimize the total distances traveled by the radio waves proved to not be effective enough.

As a result, Method 1 using only time delays failed as illustrated on Figure 4 for trajectory 105. This figure presents the projected CAMS trajectory as well as the reconstructed one in the horizontal XY plane and in the vertical XZ plane, where coordinates X,Y, and Z are given in a local Cartesian frame centered on Dourbes. It can be seen that the position of the specular reflection point for the reference station in Humain is completely wrong. The direction of the trajectory (velocity vector) is also very inaccurate although closer to the correct one. This behavior was similar for all other trajectories listed in Table 1.

Figure 5 presents the results obtained for trajectory 105 in the same horizontal and vertical planes but using Method 2. Since the direction of the reflection point is constrained via equations including the interferometer data, it is now correctly retrieved and this helps greatly the reconstruction of the trajectory. The altitude of the reflection point is still not accurate enough with an error of a few kilometers. The speed direction is accurate to  $1.5^\circ$  and the magnitude (40.7 km/s) is close to the one measured by CAMS (41.8 km/s). Note that CAMS includes a deceleration model that is not taken into account here. However, the CAMS deceleration parameters were small for trajectory 105.

Although the results are not accurate enough yet, they are encouraging. The results obtained with Method 2 for all 12 trajectories considered for this study are presented in Figure 6. Trajectory 105 is on the right side of this figure. The conclusions for most of the trajectories are identical to those presented for trajectory 105: velocity magnitude and direction are rather close to the CAMS measurements. The altitude of the reconstructed reflection point is slightly different from the position calculated on the CAMS trajectory. This difference depends on the elevation of the specular reflection point.

## 6 Discussions and perspectives

Method 1 is very important since it is the only one that can be applied to all archived BRAMS data of the

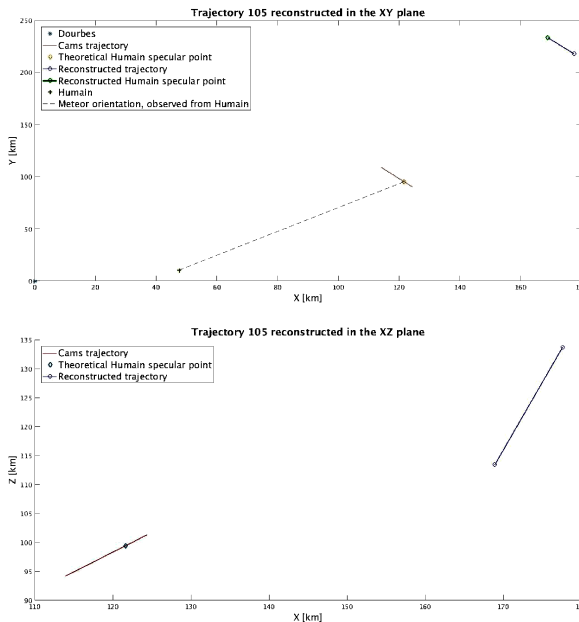


Figure 4 – Example of result obtained for CAMS trajectory 105 using Method 1.

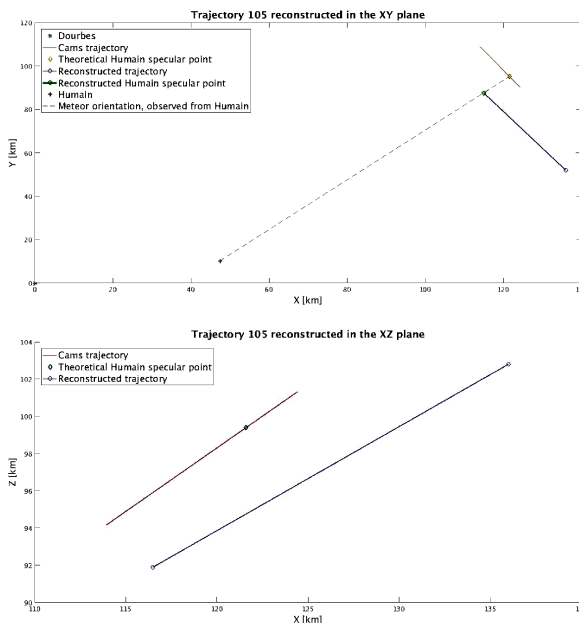


Figure 5 – Example of result obtained for CAMS trajectory 105 using Method 2.

last 10 years. Improvements such as the use of a more appropriate solver, the use of a better target objective, etc, have been considered since the IMC2021 and will be presented in a forthcoming paper. Method 2 works already much better, even at this stage of development, but cannot be applied to a lot of data since it requests to have at least 3 stations detecting the same meteor as the interferometer located in Humain. The number of receiving stations close to Humain is rather low and priority will be given to searching new locations nearby to welcome future BRAMS stations. Another priority will be to install new receiving stations to create lo-

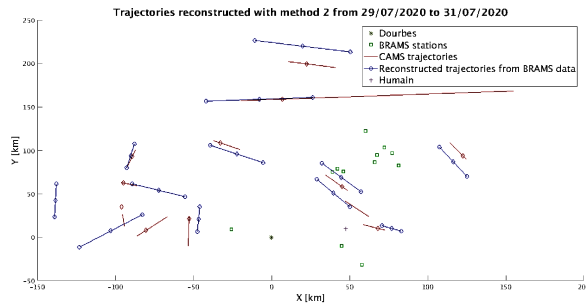


Figure 6 – Results obtained for the 12 selected CAMS trajectories using Method 2. The projections are shown in the horizontal XY plane. The position of the interferometer in Humain is indicated by the plus symbol.

cal clusters of stations as we did in 2020 in the Limburg province (North-East of Belgium). Indeed, since Method 1 requires at least 6 stations but preferably more, we need stations located not too far away from each other (in order to detect the same meteors) but not too close either (otherwise the time delays become very small and of the order of the measurement uncertainty). A spatial separation of the order of 10–30 km is therefore adequate.

Finally, we have considered another possibility for the future: including some sort of phase-coding in the transmitted CW signal in order to be able to access the total range traveled by the radio wave (see e.g. Vierinen et al., 2016). It is out of the scope of this paper to discuss the feasibility and potential complications of implementing this technique in the BRAMS network but simulations have been conducted to see what would be the advantages for meteoroid trajectory reconstruction. In this case, one additional equation describing the total distance traveled by the radio wave would become available for each receiving station. Therefore, data from only 3 stations would be enough since we would have 6 equations for 6 unknowns with the 3 equations providing  $dS_i/dt = 0$ . This was tested for the 12 selected trajectories (using the same solver) and results are presented in Figure 7. The reconstructed trajectories are very close or sometimes overlap with the CAMS ones. The reconstructed speeds are also in very good agreement with the CAMS measurements.

In conclusion, implementing a method to obtain the total range (e.g. using a CW phase coding) would certainly be of great benefit in the future but the technical implementation and subsequent data analysis is not trivial. Nevertheless, a lot of effort and development are currently made on methods 1 and 2 since they can be applied to a lot of current and archived BRAMS data. The results will be presented in another publication. Further development, improvement and extension of the BRAMS network are also constantly envisaged.

## 7 Acknowledgement

The authors would like to warmly thank Mr. Mathias Van den Bossche who worked on this topic with great motivation during his Master Thesis at the University of Liège. The BRAMS network is funded partly by

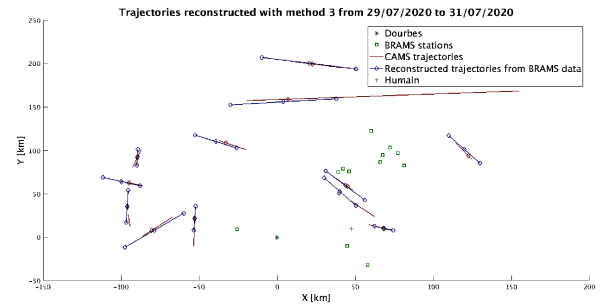


Figure 7 – Results obtained for the 12 selected CAMS trajectories using an hypothetical method where the range traveled by the radio waves would be available for each receiving station.

the Solar-Terrestrial Center of Excellence (STCE). The BRAMS project is an active Pro-Am collaboration. We would like to thank all operators hosting the receiving stations.

## References

- Anciaux M., Lamy H., Martinez Picar A., Ranvier S., Calders S., Calegario A., and Verbeeck C. (2020). “The BRAMS receiving station v2.0”. In Pajer U., Rendtel J., Gyssens M., and Verbeeck C., editors, *Proceedings of the International Meteor Conference, Bollmannsruh, Germany, 03-06 October 2019*. International Meteor Organization, pages 39–42. ISBN 978-2-87355-033-2.
- Jenniskens P., Gural P., Grigsby B. J., Newman K. E., Borden M., Koop M., and Holman D. (2011). “CAMS : Cameras for allsky meteor surveillance to establish minor meteor showers”. *Icarus*, **216**, 40–61. doi: 10.1016/j.icarus.2011.08.012.
- Jones J., Webster R., and Hocking W. (1998). “An improved interferometer design for use with meteor radar”. *Radio Science*, **33**, 55–65. doi: 10.1029/97RS03050.
- Lamy H., Anciaux M., Ranvier S., Calders S., Gamby E., Martinez Picar A., and Verbeeck C. (2015). “Recent advances in the BRAMS network”. In Rault J.-L. and Roggemans P., editors, *Proceedings of the International Meteor Conference, Mistelbach, Austria, 27-30 August 2015*. International Meteor Organization, pages 171–175. ISBN 978-2-87355-029-5.
- Lamy H. and Tétard C. (2016). “Retrieving meteoroids trajectories using BRAMS data : preliminary simulations”. In Roggemans A. and Roggemans P., editors, *Proceedings of the International Meteor Conference, Egmond, the Netherlands, 2-5 June 2016*. pages 143–147. ISBN 978-2-87355-030-1.
- Lamy H., Tétard C., Anciaux M., Ranvier S., Martinez Picar A., Calders S., and Verbeeck C. (2018). “First observations with the BRAMS radio interferometer”. In Gyssens M. and Rault J.-L., editors, *Proceedings of the International Meteor Conference, Petnica, Serbia, 21-24 September, 2017*.

International Meteor Organization, pages 132–137.  
ISBN 978-2-87355-031-6.

Mazur M., Pokorny P., Brown P., Weryk R., Vida D., Schult C., Stober G., and Agrawal A. (2020). “Precision measurements of radar transverse scattering speeds from meteor phase characteristics”. *Radio science*, **55**, 1–32. doi: 10.1029/2019RS006987.

Roggemans P., Johannink C., and Breukers M. (2016). “Status of the CAMS-BeNeLux network”. In Roggemans A. and Roggemans P., editors, *Proceedings of the International Meteor Conference, Egmond, the Netherlands, 2-5 June 2016*. IMO, pages 254–260.

Vierinen J., Chau J., Pfeffer N., Clahsen M., and Stober G. (2016). “Coded continuous wave meteor radar”. *Atmospheric Measurement Techniques*, **9**, 829–839.

---

*Handling Editor:* Javor Kac

This paper has been typeset from a L<sup>A</sup>T<sub>E</sub>X file prepared by the authors.